

## “ETCHABILITY” OF ION TRACKS IN SiO<sub>2</sub>/SI AND Si<sub>3</sub>N<sub>4</sub>/SI THIN LAYERS

Liudmila A. Vlasukova<sup>1\*</sup>, Fadei F. Komarov<sup>1</sup>, Vera N. Yuvchenko<sup>1</sup>,  
Vladimir A. Skuratov<sup>2</sup>

1 Belarusian State University, Nezaleznosti Ave. 4, 220030, Minsk, Belarus

2 Laboratory of Nuclear Reactions, Joint Institute for Nuclear Research, 141980, Dubna, Russia

### ABSTRACT

We have calculated radii and lifetime of the molten regions or the regions heated to the melting point that are formed under irradiation of amorphous SiO<sub>2</sub> and Si<sub>3</sub>N<sub>4</sub> with swift ions. A computer simulation was carried out on the base of thermal spike model. A comparison of calculated track parameters with ion track etching data have been made for these materials.

It is shown that an existence of molten region along swift ion trajectory may be a criterion for a track “etchability” in the case of SiO<sub>2</sub>. In the same conditions of chemical etching diameter of etched tracks in SiO<sub>2</sub> is proportional to the radius and lifetime of the molten region. This information is important for a correct choice of irradiation regime aimed at preparation of nanoporous layers with high pore density ( $\geq 10^{10}$  cm<sup>-2</sup>).

**Key words:** SiO<sub>2</sub> и Si<sub>3</sub>N<sub>4</sub>, swift ions, ion tracks, chemical etching, nanoporous layers.

### INTRODUCTION

The discovery of ion tracks dates back to 1959 when Silk and Barnes published transmission electron micrographs of mica with long, straight damage trails created by single fragments from the fission of <sup>235</sup>U [1]. Soon after that, it has been realized that ion tracks are narrow (<5 nm), stable, chemically reactive centers of strain that are composed mainly of displaced atoms rather than of electronic defects [2]. It also became clear that these displaced atoms are not due to direct collisions between ions and the target nuclei, but are the result of the interaction of the projectile ions with the target electrons. Later it was found that tracks were formed in insulators and badly conducting semiconductors, if the electronic stopping power  $S_e$  exceeded a material-dependent threshold value  $S_{e0}$ . At that time no tracks could be detected in metals [3]. Nanochannels can be created in track regions by means of proper chemical etching. Thin dielectric layers (SiO<sub>2</sub> and Si<sub>3</sub>N<sub>4</sub>) with the etched tracks integrated into silicon wafers are of special interest for nanotechnologies and microelectronics [4 – 8]. A material-dependent threshold value  $S_{e0}$  is often treated as a criterion for ion

---

\* e-mail: vlasukova@bsu.by, tel: (+375)0172095929

track “etchability”.  $S_{e0}$  varies from 4 to 1.5 keV/nm for SiO<sub>2</sub> according different Refs [2, 9 - 11]. There is practically no information about  $S_{e0}$  for silicon nitride in literature. We know three papers only that devoted to track investigation in this material [12 - 14]. Though, in addition to  $S_{e0}$  it is necessary to know track parameters in order to obtain dielectric layers with the definite nanopore density by means of swift ion irradiation followed by chemical etching.

In this paper, we evaluate a possibility to use track formation parameters calculated on the base of thermal spike as criterions for ion track “etchability” in amorphous SiO<sub>2</sub> and Si<sub>3</sub>N<sub>4</sub> layers.

### **METHODS OF SAMPLE MANUFACTURING AND ANALYSIS**

SiO<sub>2</sub>/Si samples were cut from the thermally oxidized Si wafer. The thickness of SiO<sub>2</sub> layer was evaluated from RBS measurements and equal to 600 nm. Si<sub>3</sub>N<sub>4</sub>/Si samples were cut from the Si wafer with the amorphous silicon nitride layer deposited by gas phase low pressure deposition from ammonia and dichlorosilane at 300° C. The Si<sub>3</sub>N<sub>4</sub> layer thickness measured by the Rutherford backscattering method was 600 nm, too. SiO<sub>2</sub>/Si and Si<sub>3</sub>N<sub>4</sub>/Si structures were irradiated normally to the surface with Ar (290 MeV), Fe (56 MeV), Kr (84 MeV), and W (180 MeV) ions in the Flerov Laboratory of Nuclear Reactions of the Joint Institute for Nuclear Research (Dubna). The ion fluence in all cases did not exceed  $5 \times 10^8 \text{ cm}^{-2}$ . The ion flux was kept constant and equal to  $2 \times 10^8 \text{ cm}^{-2} \text{ s}^{-1}$ . To provide reliable thermal contacts the samples were fixed on a massive metallic holder with a heat conducting paste. The irradiated samples were treated in hydrofluoric acid (HF) dilute aqueous solutions at room temperature. Then the samples were investigated using the scanning electron microscope Hitachi S-4800.

### **THE COMPUTER SIMULATION OF THE TRACK FORMATION IN SILICON DIOXIDE AND NITRIDE IN TERMS OF THERMAL SPIKE**

The track formation processes in amorphous SiO<sub>2</sub> ( $\alpha$ -SiO<sub>2</sub>) and Si<sub>3</sub>N<sub>4</sub> were simulated in terms of the thermal spike model [15] with the application of a software system we designed. The model was successfully used earlier to describe swift ion travel in silicon dioxide and other dielectrics. The track radii in  $\alpha$ -SiO<sub>2</sub> we computed by this model were in good agreement with the experimental results in [16, 17]. The model involves the thermalization of the electronic subsystem of a solid within a time not exceeding  $10^{-14}$  s. A few picoseconds later, the electron–phonon interaction leads to fast heating of the region along the fast ion trajectory. The process of energy transfer from the electronic to atomic subsystem of a solid is described by a system of two differential equations. The macroscopic parameters of the target material are used to calculate thermal fields. The model involves one free parameter: the electron mean free path under electron–phonon interaction  $\lambda$ . If the density of the energy released in electronic excitations is sufficiently high, we observe the melting of

the material and the formation of a cylindrical domain with a diameter of a few nanometers - the future track. A few tens of picoseconds later, the melt cools to the temperature of the surrounding matrix.

The thermophysical parameters for SiO<sub>2</sub> were taken from [15], the parameter  $\lambda$  was 4 nm. For Si<sub>3</sub>N<sub>4</sub> the parameter  $\lambda$  was 4.8 nm [15]. Thermophysical properties of amorphous SiO<sub>2</sub> - one of the basic materials of microelectronic processing - are thoroughly studied and described in the literature. The situation is different for amorphous Si<sub>3</sub>N<sub>4</sub>. We failed to find reference data on latent heat of melting of this material. In addition, distillation or thermal decomposition of the material can take place upon the heating of Si<sub>3</sub>N<sub>4</sub>, along with solid phase melting. Therefore, as a track region in Si<sub>3</sub>N<sub>4</sub> we took the region heated to the melting point instead of the melted region. The latent heat of melting of Si<sub>3</sub>N<sub>4</sub> was taken to be 10<sup>8</sup> J kg<sup>-1</sup>, which is higher by two orders of magnitude than average values of semiconductors.

## RESULTS AND DISCUSSION

Table 1 presents the results of computer simulation of ion track formation, namely, the radius and lifetime of molten region for SiO<sub>2</sub> and Si<sub>3</sub>N<sub>4</sub>.

**Table 1** – The results of computer simulation for SiO<sub>2</sub> and Si<sub>3</sub>N<sub>4</sub>

Material	Ion type and energy, MeV	The electronic stopping power $S_e$ , keV/nm	The radius of the molten region $r^{**}$ , nm	The lifetime of the molten region $t^{**}$ , ps
SiO <sub>2</sub>	Ar (290)	2.8	-	-
	Kr (253)	9.8	3.4	7.0
	Kr (84)	9.4	3.8	8.9
	W (180)	15.8	6.3	24.4
	Fe (56)	6.9	2.7	3.9
Si <sub>3</sub> N <sub>4</sub> ***	W (180)	20.4	5.3	4.7
	Kr (84)	11.9	3.0	1.3
	Fe (56)	9.0	1.7	0.5

\*  $S_e$  were calculated by SRIM' 2003 code

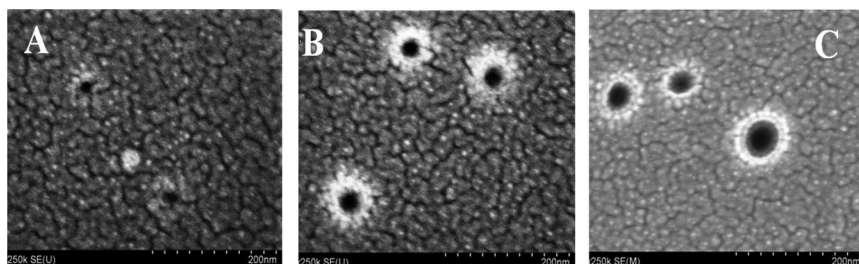
\*\* for Si<sub>3</sub>N<sub>4</sub> the parameters  $r$  and  $t$  are the radius of the region heated to the melting point and the lifetime of this region, accordingly

\*\*\* the density of Si<sub>3</sub>N<sub>4</sub> was taken to be 2.85 g cm<sup>-3</sup> [18] for  $S_e$  calculation

In the case of Ar (290 MeV)  $S_e$  is equal to 2.8 keV/nm. It is higher than the threshold value for the preferential track etching reported in [10, 11]. One can see that in the case of SiO<sub>2</sub> irradiation with Ar ions (290 MeV) there is no formation of molten region along the ion trajectory. Accordingly, we did not found the etched tracks in the SiO<sub>2</sub>/Si samples irradiated with Ar even after the treatment in 6% HF for 20 minutes. Evidently, in order to forecast the "etchability" of ion tracks it is not enough to know  $S_e$  only. We have to take into account "velocity effect" [19]. In our calculation this effect is demonstrated for

SiO<sub>2</sub> irradiated with Kr ions with the energies of 253 and 84 MeV. For Kr (253 MeV) the electronic stopping power is 9.8 keV/nm. This is higher than a value 9.4 keV/nm for Kr (84 MeV). However, the radius and the lifetime of the molten region are larger in the case of slower ion. In the conditions of similar  $S_e$  the most part of released energy is localized in narrow regions along ion trajectories during slow ions passing. During swift ion passing a substantial part of energy goes away from the ion trajectory for significant distances with high-energy  $\delta$ -electrons. Thus, a substance temperature in the region of future track ought to be higher in the case of slow ion passing. Evidently, the molten region formation along ion trajectory is more reliable criterion for track “etchability” in comparison with  $S_e$ . Figure 1 shows images of etched tracks in SiO<sub>2</sub>/Si samples irradiated with Fe, Kr and W ions and chemically treated in the same conditions.

One can see from *Fig. 1* that tracks were etched in all samples. It should be noted a correlation between etched pore diameters and calculated radii and lifetimes of the molten regions. Pore diameter in SiO<sub>2</sub> irradiated with Fe ions was  $\approx$  15 nm after the etching in 1.5% HF solution during 9 min. For the samples irradiated with Kr and W ions pore diameters were 30 and 45 nm, accordingly. Thus, the smallest pore diameter was observed for silicon dioxide irradiated with ions that formed molten regions with small radii and lifetime. The biggest one was observed in the case of W irradiation. According to our calculation W ions created the biggest molten regions with the longest lifetime from three ion species used in our experiment. Earlier for  $\alpha$ -SiO<sub>2</sub> irradiated with Bi (710 MeV) it was shown a good correlation between minimum etched tracks diameters and molten region radii calculated by thermal spike [17]. In this way, one can forecast minimum etched tracks diameters on the base of the molten region radius knowledge. It is important for a choice of proper irradiation regime aimed at preparation of nanoporous layers with high pore density ( $\geq 10^{10}$  cm<sup>-2</sup>).



Irradiated samples were treated in 1.5% HF for 9 min.

**Fig. 1** – Etched tracks in SiO<sub>2</sub>. A – irradiation with Fe (56 MeV,  $2.4 \times 10^8$  cm<sup>-2</sup>), B – Kr (84 MeV,  $2.4 \times 10^8$  cm<sup>-2</sup>), C – W (180 MeV,  $3 \times 10^8$  cm<sup>-2</sup>)

As analysis of calculated track parameters shows, a region heated to the melting point exists during the irradiation with all three ion species in the case of  $\text{Si}_3\text{N}_4$ .

Though, track formation process needs more energy spend in comparison with  $\text{SiO}_2$ . At more high level of the electronic stopping power in  $\text{Si}_3\text{N}_4$  for Fe, Kr and W ions the calculated lifetime of the region heated to the melting point were substantially shorter in comparison with the lifetime of the molten region for  $\text{SiO}_2$ .

In the  $\text{Si}_3\text{N}_4/\text{Si}$  samples irradiated with Fe and Kr, no tracks were revealed even after 60 min treatment in an HF solution. Tracks were etched only upon exposure to W ions. *Figure 2* depicts the scanning electron microscope image of the W irradiated sample after etching. Ten pores were recorded on a scan area of  $7.8 \times 5.5 \mu\text{m}^2$ . The track etching efficiency, defined as  $\xi = N_p/\Phi$ , where  $N_p$  is the number of pores per unit area and  $\Phi$  is the fluence, did not exceed 12%. The low track etching efficiency and the considerable difference in the diameters of the etched pores allow us to assume that discontinuous tracks are formed in silicon nitride upon irradiation with tungsten (180 MeV). This means that the electronic stopping power of W ions are sufficient for order–disorder transformation; however, they are lower than the threshold electron losses necessary for the formation of extended etched tracks in this material. This conclusion on the formation of discontinuous tracks in amorphous  $\text{Si}_3\text{N}_4$  irradiated with lead ions with  $S_e = 19.3 \text{ keV/nm}$  was also drawn by Canut et al. [13]. They reported about track etching efficiency  $\xi = 60\%$  with an appreciable size spread of pores.

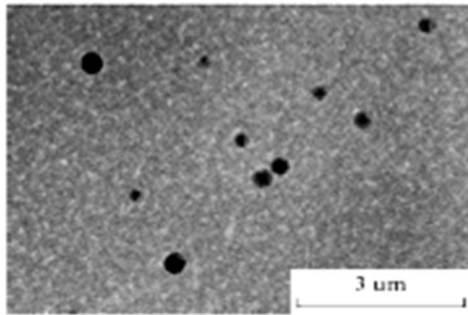


**Fig. 2** - Scanning electron microscope image of  $\text{Si}_3\text{N}_4$  surface irradiated with W ions (180 MeV,  $2 \times 10^8 \text{ cm}^{-2}$ ) and etched in 4% HF for 50 min

To obtain nanoporous  $\text{Si}_3\text{N}_4$  with the pore density controlled by ion fluence, the formation of extended continuous tracks is required. This condition can be fulfilled with the use of ions with  $S_e > 20 \text{ keV/nm}$ .

According to computer simulation data the regions heated to the melting point exist in  $\text{Si}_3\text{N}_4$  during the irradiation with all three ion species (Fe, Kr and W). Though, chemical treatment results show the preferential etching of discontinuous tracks only for the samples irradiated with tungsten. This ion type is characterized with the maximal energy losses in electron subsystem for our experiment. Probably, we have done incorrect assumptions in computer simulation of track

formation in  $\text{Si}_3\text{N}_4$  because the absence of reliable data on thermophysical properties of this material. A fitting of thermal spike model in application to amorphous  $\text{Si}_3\text{N}_4$  is a subject of further investigation.

### CONCLUSIONS

The radii and lifetime of the molten regions or the regions heated to the melting point formed in amorphous  $\text{SiO}_2$  and  $\text{Si}_3\text{N}_4$  irradiated with swift ions have been calculated on the base of thermal spike model. A comparison of calculated track parameters and etching of ion track data have been made for these materials.

It is shown that an existence of molten region along swift ion trajectory may be used as a criterion for track “etchability” in the case of  $\text{SiO}_2$ . In the same conditions of chemical etching diameter of etched tracks in  $\text{SiO}_2$  is proportional to the radius and lifetime of the molten region. This information is important for a correct choice of irradiation regime aimed at preparation of nanoporous layers with high pore density ( $\geq 10^{10} \text{ cm}^{-2}$ ).

As a computer simulation shows, in the case of irradiation with Fe (56 MeV), Kr (84 MeV), and W (180 MeV) at more high level of the electronic stopping power in  $\text{Si}_3\text{N}_4$  the calculated lifetime of the region heated to the melting point were substantially shorter in comparison with the calculated lifetime of the molten region for  $\text{SiO}_2$ .

In silicon nitride irradiated with swift ions, tracks were etched only after exposure to W ions (180 MeV) with  $S_e = 20 \text{ keV/nm}$  being maximal for our experiment. The low track etching efficiency and the considerable size spread of pores allow assuming the formation of discontinuous tracks.

An existence of the regions heated to the melting point along swift ion trajectory can not be used as a criterion for track “etchability” in the case of  $\text{Si}_3\text{N}_4$ . It needs an additional investigation for a fitting of thermal spike model in application to amorphous  $\text{Si}_3\text{N}_4$ .

### Acknowledgements

This work was supported by the Belarusian Foundation for Basic Research, grant T10R–142.

### REFERENCES

- [1] E.C.H. Silk, R.S. Barns, *Philos. Mag.*, 1959, Vol.4, P.970.
- [2] *Nuclear Tracks in Solids* (Eds. R.L. Fleischer, P.B. Price, R.M. Walker) University of California Press, Berkeley, 1975.
- [3] S. Klaumünzer, *Nucl. Instr. and Meth.*, 2004, Vol. B225, P. 136 - 153.
- [4] M. Toulemonde, C. Trautman, E. Balanzat *et al*, *Radiat. Measurements*, 2005, Vol. 40, P. 191.
- [5] K. Hoppe, W.R. Fahrner, D. Fink *et al*, *Nucl. Instr. and Meth.*, 2008, Vol. B266, P. 1642 - 1646.

- 
- [6] F. Bergamini, M. Bianconi, S. Cristiani *et al*, Nucl. Instr. and Meth., 2008, Vol. B266, P. 2475.
- [7] M. Fujimaki, C. Rockstuhl, X. Wang *et al*, Optics Express, 2008, Vol.16, P. 6408.
- [8] N. Fertig, R. H. Blick, J. C. Berhends, Biophysical J. 2002, Vol. 18, P. 3056 - 3062.
- [9] A. Sigrist, R. Balzer, Helv. Phys. Acta, 1977, Vol. 50, P.75.
- [10] J. Jensen, M. Skupinski, A. Razpet, G. Possnert, Nucl. Instr. and Meth., 2006, Vol. B245, P. 269 - 273.
- [11] A. Dallanora, T. L. Marcondes, G. G. Bermudez *et al*, J. Appl. Phys., 2008, Vol. 104, P. 024307(8).
- [12] S. J. Zinkle, V. A. Skuratov, D. T. Hoelzer, Nucl. Instr. and Meth., 2002, Vol. B191, P. 758.
- [13] B. Canut, A. Ayari, K. Kaja *et al*, Nucl. Instr. and Meth., 2008, Vol. B266, P. 2819 - 2823.
- [14] L.A. Vlasukova, F.F. Komarov, V.N. Yuvchenko, Bulletin of the Russian Academy of Sciences: Physics, 2010, Vol. 74, P. 206 – 208.
- [15] M. Toulemonde, C. Dufour, A. Meftah, E. Paumier, Nucl. Instr. and Meth. 2000, Vol. B166–167. P. 903–912.
- [16] F.F. Komarov, L.A. Vlasukova, V.N.Yuvchenko *et al*, Izv. Akad. Nauk, Ser. Fiz., 2006, Vol. 70, P. 798 - 801.
- [17] F.F. Komarov, L.A. Vlasukova, P.V. Kuchinskyi *et al*, Lithuanian J. Phys., 2009, Vol. 49, P. 111 - 115.
- [18] Gmelin Handbook on Inorganic and Organometallic Chemistry, Springer–Verlag, 1994, vol. B5e, p. 264.
- [19] A. Meftah, F. Brisard, J. M. Costantini *et al*, Phys. Rev. B., 1994, Vol. 49, P. 12457 - 12463.